Available online at www.sciencedirect.com

ScienceDirect

Procedia Engineering 147 (2016) 32 – 37

Procedia Engineering

www.elsevier.com/locate/procedia

11th conference of the International Sports Engineering Association, ISEA 2016

Wind-tunnel experiments and trajectory analyses for five nonspinning soccer balls

John Eric Goff[a,*], Chad Michael Hobson[a], Takeshi Asai[b], Sungchan Hong[b]

[a] *Lynchburg College, Department of Physics, Lynchburg, VA, 24501, USA*
[b] *University of Tsukuba, Institute of Health and Sports Science, Tsukuba-city, 305-8574, Japan*

Abstract

We report drag, side, and lift coefficients for two orientations of five non-spinning soccer balls (Brazuca, Cafusa, Jabulani, Teamgeist 2, and Vantaggio), measured using a wind tunnel. The air's speed range was 7 m/s to 35 m/s, covering most of the speeds of kicked soccer balls in real games. Trajectory analyses make use of our aerodynamic wind-tunnel data and show that the five balls we tested behave differently while in flight. We also show that in some cases, changing ball orientation leads to a significant change in flight trajectory. Turning off side and lift forces alter ranges and lateral deflections as fractions of ranges in excess of 10% for some balls. Because we have only two orientations for non-spinning balls, the work we present here is just the preliminary investigation of a much larger project in which we hope to have aerodynamic data for many more ball orientations.

Peer-review under responsibility of the organizing committee of ISEA 2016
Keywords: aerodynamics; soccer; Association football; trajectory analysis; wind tunnel

1. Introduction

We recently published work [1] on wind-tunnel measurements of drag coefficients for non-spinning Jabulani and Brazuca soccer balls, which were the balls used in the past two World Cups. With the help of trajectory analysis, our study showed that Brazuca is a much better ball than Jabulani. Each World Cup has a new soccer ball, so an understanding of ball aerodynamics helps players, researchers, and manufacturers learn what works on a given ball, and what does not work. Jabulani was made by Adidas and used in South Africa for the 2010 World Cup. The reduction from the 14 thermally-bonded panels of the Teamgeist ball used in the 2006 World Cup to the eight thermally-bonded panels of the Jabulani ball meant Adidas had to texture Jabulani's panels to provide enough surface roughness so that the ball would not behave too differently from previous balls. Jabulani ultimately met with controversy because of poor performance [2,3]. Brazuca performed better in Brazil in 2014, partly explained in our aforementioned work [1].

More of our recent work [4,5] has been dedicated to understanding surface effects, including seam length, on aerodynamics for a variety of soccer balls. Though we published a few numerically-determined trajectories in two dimensions in that recent work, we did not evaluate full three-dimensional trajectories determined by drag, side, and

* Corresponding author. Tel: +1-434-544-8856 ; fax: +1-434-544-8646.
E-mail address: goff@lynchburg.edu

Peer-review under responsibility of the organizing committee of ISEA 2016
doi:10.1016/j.proeng.2016.06.185

lift forces. We follow up on our previous work with a much more substantial effort here, highlighted by complete trajectory analyses of five different soccer balls, each in two different orientations, using aerodynamic coefficients determined in our wind tunnel. Our trajectory analyses are presented over a full range of launch speeds, 15 m/s to 35 m/s. We show here that altering the orientation of a non-spinning ball can significantly influence the ball's trajectory.

Four of the balls we studied are made by Adidas: Brazuca (six panels with small dimples), Cafusa (32 panels with small drip texture), Jabulani (eight panels with small ridges), and Teamgeist 2 (14 panels with small bumps). We also tested a ball made by Molten: Vantaggio (32 panels with smooth texture). All balls have the same diameter, $D = 0.22\,\mathrm{m}$, but their masses are different: Brazuca with $m = 0.432\,\mathrm{kg}$, Cafusa with $m = 0.437\,\mathrm{kg}$, Jabulani with $m = 0.438\,\mathrm{kg}$, Teamgeist 2 with $m = 0.431\,\mathrm{kg}$, and Vantaggio with $m = 0.442\,\mathrm{kg}$.

Aerodynamics of soccer balls have been researched extensively over the past couple of decades. Numerous references to work done up through 2012 may be found in a recent review article [6] on sport aerodynamics. More work has been published by other research groups [7–10] since that review article was published.

2. Experimental Technique

Experiments were performed in a closed-circuit wind tunnel (manufactured by San Technologies Co, Ltd, Tochigi, Japan) at the University of Tsukuba. Maximum flow speed of this wind tunnel is 55 m/s. The blower outlet is 1.5 m × 1.5 m; flow speed distribution is within ±0.5%; and turbulence is 0.1% or less. All soccer balls tested had a diameter of 0.22 m, meaning the blockage was roughly 1.7%. We used a traditional rear-mounted technique [11], by which a soccer ball is mounted to a horizontal stainless steel rod, and horizontal air blows over the ball from the opposite direction. Figure 1 shows a Brazuca soccer ball mounted to the rod prior to testing.

We performed wind-tunnel measurements on two orientations for each ball. Of the infinite number of possible ways to orient a ball in a wind tunnel, we selected what we consider to be two considerably different orientations. By that we mean two orientations that present frontal geometries to the oncoming air with significantly different panel and seam orientations on the front and sides. Though our choices are completely subjective, we feel that we have chosen two orientations for each ball that will aid understanding in non-spin aerodynamics. Figure 2 shows photos of the various ball orientations. The orientations for each ball are labeled by A and B. Those designations are merely to distinguish ball orientations and do not represent anything similar among the five balls. Orientation A for Brazuca, for example, has nothing to do with orientation A for Jabulani.

Aerodynamic forces were measured at flow speeds in the range $7\,\mathrm{m/s} \le v \le 35\,\mathrm{m/s}$, which corresponds to a Reynolds number range of approximately $10^5 < \mathrm{Re} < 5 \times 10^5$, where $\mathrm{Re} = vD/\nu$ [12], with D the ball's diameter, and $\nu = 1.54 \times 10^{-5}\,\mathrm{m^2/s}$, the kinematic viscosity. Air forces acting on a mounted ball were measured during a 9-s time interval by a sting-type six-component force detector (model number LMC-61256 by Nissho Electric Works Co, Ltd). Data recording was done on a personal computer with an A/D converter board that has a 1000-Hz sampling rate.

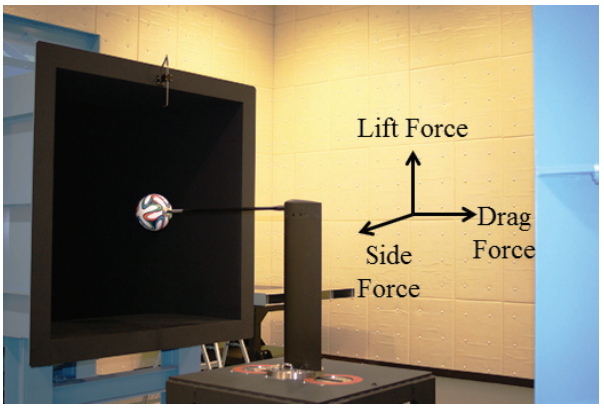

Fig. 1. Adidas Brazuca soccer ball mounted on stainless steel rod prior to wind-tunnel experiment. Axes associated with the various force directions are also shown.

Fig. 2. Photos of the two orientations, labeled A and B, that we chose for each of the five balls we tested in a wind tunnel.

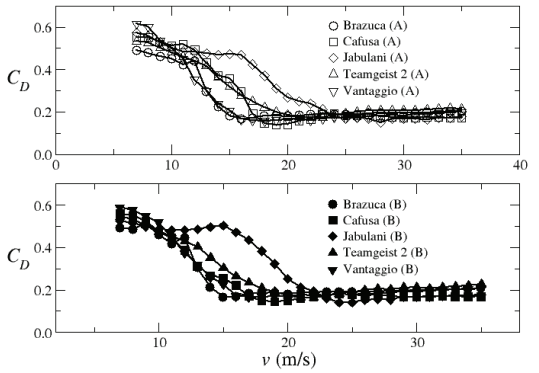

Fig. 3. Speed-dependent drag coefficients for the five balls we tested. Symbols are experimental data; lines between symbols serve to aid the eye. The top figure shows orientations A; the bottom figure shows orientations B.

Though there is just one force on a ball from the oncoming air, we follow convention [12] and separate that force into the three Cartesian components shown in Fig. 1. The drag, side, and lift forces have magnitudes given by [12]

$$F_D = \frac{1}{2}\rho A C_D v^2, \qquad F_S = \frac{1}{2}\rho A C_S v^2, \qquad \text{and} \qquad F_L = \frac{1}{2}\rho A C_L v^2, \tag{1}$$

respectively, where $A = 0.038\,\mathrm{m}^2$ is the ball's cross-sectional area, $\rho = 1.2\,\mathrm{kg/m}^3$ is air's mass density, and C_D, C_S, and C_L are the drag, side, and lift coefficients, respectively. Once force components are measured, they are averaged over the 9-s data-taking time interval, and then aerodynamic coefficients are extracted from Eq. 1. We realize that averaging force components over 9 s of data taking averages over hysteresis effects [13,14]. Extracting aerodynamic coefficients from average forces thus introduces slight errors (< 10%) into the trajectory analyses in Sec. 4.

3. Wind-Tunnel Results

Figure 3 shows C_D versus v for balls we tested in the two orientations shown in Fig. 2. For all figures, Brazuca is represented with a circle (◯), Cafusa with a square (□), Jabulani with a diamond (◇), Teamgeist 2 with an upward triangle (△), and Vantaggio with a downward triangle (▽). Open symbols refer to orientation A; closed symbols to orientation B. The precipitous rise in C_D as air speed decreases is called the drag crisis. Jabulani's drag crisis occurs at a speed larger than for the other balls, regardless of orientation. That is one reason why Jabulani experienced controversy in the 2010 World Cup; its drag crisis occurs in the speed range for intermediate-speed kicks [1].

A perfectly smooth, non-spinning ball has $C_S = 0$ and $C_L = 0$. Soccer balls have seams and possibly textured panels, leading to surfaces of nonuniform roughness, meaning that, in general, $C_S \neq 0$ and $C_L \neq 0$. Figure 4 shows wind-tunnel data for C_S and C_L versus v for each ball and each orientation. Side and lift forces arise via asymmetric shedding of the boundary layer, which means changing a ball's orientation leads to different boundary-layer shedding.

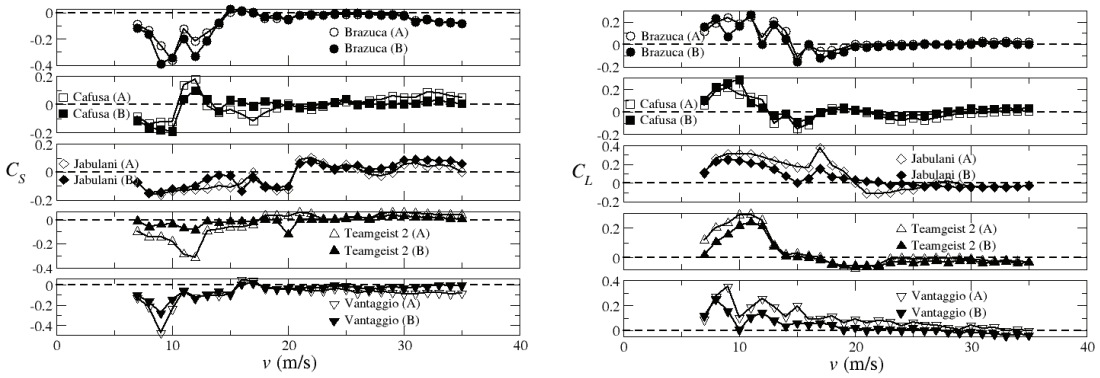

Fig. 4. Speed-dependent side (left) and lift (right) coefficients for each of the two orientations of the five balls we tested. Symbols are experimental data; lines between symbols serve to aid the eye. Horizontal dashed lines show where C_S and C_L change sign.

Altering orientations changes the curves in Fig. 4, including the speeds where signs change, as demonstrated by our choice of A and B orientations. The magnitudes of C_S and C_L do not change appreciably from one orientation to the next, meaning what we show in Fig. 4 is likely representative of C_S and C_L for our soccer balls.

Note in Fig. 4 the low-speed variance of C_S and C_L. Figure 3 shows that all balls experience a drag crisis below 20 m/s. Transitioning from laminar air flow around a ball at low speeds to turbulent air flow at high speeds may be hastened by surface roughness, whereby a rough patch on the surface trips the boundary layer [15]. As airflow around a non-spinning ball increases, rougher parts of the ball will induce transitions from laminar to turbulent flow sooner than smoother parts of the ball. That changes the asymmetric boundary-layer separation at the back of the ball, thereby changing the direction of the net transverse air force on the ball. Though all balls show appreciable C_S at low speeds, Jabulani shows the largest C_S at high speeds, illustrating partially why Jabulani was criticized for wild knuckling effects at high speeds in the 2010 World Cup [16]. An example of such a kick was the free kick by Japan's Keisuke Honda against Denmark in the 17th minute on 24 June 2010 [17].

All balls show significant C_L at low speeds, yet insignificant C_L at high speeds. The sizes of C_S and C_L are comparable to what spinning balls have [18]. The results in Fig. 4 may be interchanged by rotating balls by 90° about an axis through the support rod because the mechanism for the side and lift components of the air force is the same.

4. Trajectory Comparisons

We now describe implications of the wind-tunnel results on soccer ball trajectories. To use the wind-tunnel results presented in the previous section, we assume all soccer balls are kicked with no spin and in one of the two orientations in Fig. 2. What we present in this section is thus representative of an infinite number of possible starting orientations. We further assume that the orientation of the ball does not change while in flight.

Our model ball of mass m is kicked such that its initial launch velocity has magnitude v_0 and points at angle θ_0 with the horizontal. While in the air, the ball is subject to forces from air and Earth. We ignore the buoyant force on the ball, which is about 1.5% of the ball's weight, and consider the air's force on the ball to have the three components given by Eq. 1. The drag force, with magnitude F_D, points opposite the ball's velocity. The side force, with magnitude F_S, points parallel to the ground and perpendicular to the ball's velocity. The side force is responsible for lateral deflections. The lift force, orthogonal to both the drag and side forces, is also perpendicular to the ball's velocity, and lies in the plane formed by the ball's velocity and the ball's weight. Newton's second law equation thus gives

$$m\,\frac{d^2\vec{r}(t)}{dt^2} = \vec{F}_D + \vec{F}_S + \vec{F}_L + m\,\vec{g}\,, \tag{2}$$

where $\vec{g}$ is the acceleration due to gravity, points down, and has magnitude $g = 9.8\,\mathrm{m/s^2}$. Separating the above equation into three Cartesian components is straightforward [19], so we spare the reader the details. The numerical solution to Eq. 2 gives $\vec{r}(t)$, the time-dependent position vector of the ball with respect to the origin at the launch point.

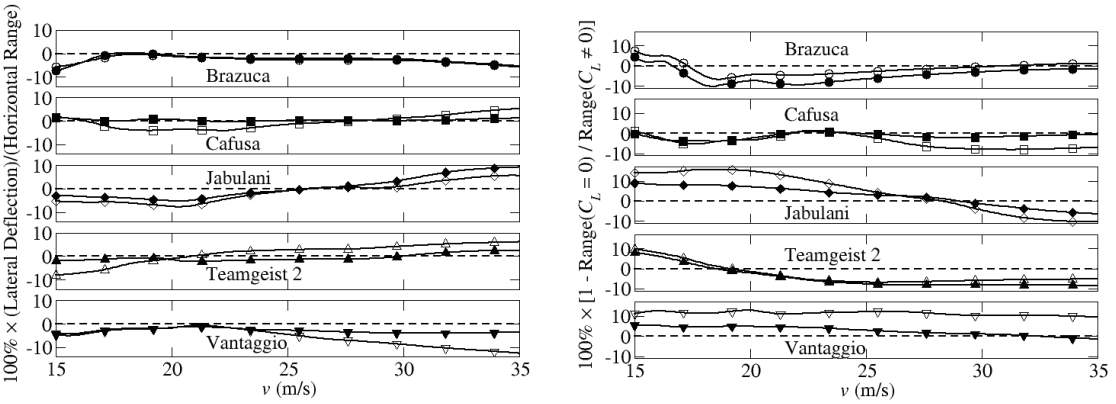

Fig. 5. Lateral deflection as a percentage of horizontal range (left) and percent change in horizontal range for $C_L = 0$ (right) for each orientation of the five balls tested. The launch angle for all kicks was $\theta_0 = 25°$. Symbols on the curves serve only to label them. All vertical axes on the left run from -14% to 10%; those on the right run from -11% to 17%.

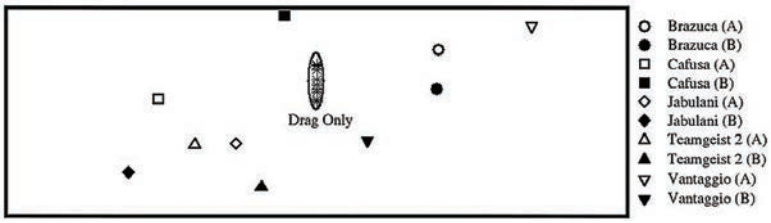

Fig. 6. Locations where the non-spinning balls in both orientations would cross the goal plane. They all start 35 m from the goal's center; $v_0 = 35\,\mathrm{m/s}$ and $\theta_0 = 13°$. We show where the balls would cross the goal plane if $C_S = 0$ and $C_L = 0$ (given by $*$).

For the aerodynamic coefficients, C_D, C_S, and C_L, we use linear interpolation between the data provided by our wind tunnel. With lines between data points, the speed-dependent aerodynamic functions are as they appear in Figs. 3–4.

Figure 5 shows the amount of lateral deflection as a percentage of the horizontal range for each orientation of each ball as a function of launch speed. The launch angle for all kicks was $\theta_0 = 25°$. Note that when the percentage in Fig. 5 reaches zero, as it does for both orientations of Jabulani at a launch speed of about 26 m/s, the implication is that the ball has moved laterally in one direction, only to move back as the ball slows and the sign of C_S changes.

Cafusa and Teamgeist 2 show the smallest lateral deflection over the range of speeds we modeled. For high-speed kicks, it is perhaps not surprising that Jabulani shows the greatest lateral deflection as a percentage of its horizontal range at nearly 10% for $v_0 = 35\,\mathrm{m/s}$ when looking at both orientations. Vantaggio shows a high-speed lateral deflection of almost 14% when in orientation A. What is seen in Fig. 5 is, as expected, consistent with Fig. 4. For example, Cafusa's side coefficient in orientation A is larger than it is while the ball is in orientation B. Figure 5 shows Cafusa's orientation A giving a larger lateral deflection than its orientation B.

Figure 5 also shows the percent change in the horizontal range when $C_L = 0$. The launch angle for all kicks is again $\theta_0 = 25°$. For high-speed kicks, Teamgeist 2 has the greatest change in the range when lift is turned off, a nearly 11% change for $v_0 = 35\,\mathrm{m/s}$ while in orientation A. The reason the Teamgeist 2 curve flattens out for high-speed kicks can be found in Fig. 4. The value of C_L for high speeds is essentially constant. The fact that Jabulani has the largest C_L values at low speeds explains why it has the largest percent change in range when lift is turned off. Figure 5 is consistent with Fig. 4 as, for example, larger lift coefficients for Vantaggio's orientation A compared to orientation B lead to larger values in Fig. 5.

We now model a long free kick, originating 35 m away from the center of the goal. Balls are kicked spinless at $v_0 = 35\,\mathrm{m/s}$ and $\theta_0 = 13°$, and in each of the two orientations. We chose those launch conditions so that all five balls in either orientation result in goals. Figure 6 shows where each of the five balls in each of the two orientations passes through the goal plane. Figure 6 also shows where the balls in each orientation would cross the goal plane if $C_S = 0$

and $C_L = 0$, i. e. drag-only trajectories. Note the large effect of side and lift forces on Jabulani in orientation B and Vantaggio in orientation A. The reason a ball passes the goal plane higher than it would have had side and lift forces been turned off is that it has $C_L > 0$ for high speeds. As seen in Fig. 4 for Brazuca and Vantaggio in orientation A and Cafusa in orientation B, balls enter the goal plane higher than their corresponding drag-only trajectories.

5. Conclusions

We reported a complete aerodynamics profile for two orientations of five non-spinning soccer balls: Brazuca, Cafusa, Jabulani, Teamgeist 2, and Vantaggio. Two of the balls, Cafusa and Vantaggio, have 32 panels, which create more uniformly rough surfaces. Though texturing the panels of new balls helps roughen the surface enough to ensure a drag crisis consistent with older balls, the reduction in total seam length leads to greater chance for asymmetric boundary-layer separation, which means greater side and lift forces. The exception to the previous comment is Jabulani, which has a drag crisis at a speed higher than for all other balls we tested.

We showed that the inclusion of side and lift forces creates trajectories with lateral deflections in excess of 10% of the horizontal range for the A orientation of Vantaggio and about 10% for the B orientation of Jabulani. All balls showed range changes as large as about 10% for various launch speeds and orientations.

The effects we describe in this paper fall under the classification of knuckling effects, but balls that baffle goal keepers that are referred to as "knuckling" typically have a small amount of spin. That is what makes a knuckleball effective in baseball. As the ball rotates, the direction of the asymmetric boundary-layer separation changes, which is why the ball wobbles along its trajectory. We do not report wobbling effects in this work because the five balls we tested had a single orientation while in our wind tunnel. Though the magnitudes of C_S and C_L do not vary much from what we reported here as orientations change, their signs will change as balls go through different orientations.

Our future goal is to obtain more complete aerodynamic profiles of the five balls we tested. That will allow us to more accurately model trajectories for balls with small spin, and thus show knuckling effects, adding on to previous work [22,23]. Though the two orientations we used for each ball give us reasonable representations of flow patterns, we need more data from other orientations to determine aerodynamic coefficients as functions of ball orientation.

References

[1] Goff JE, Asai T, and Hong S. A comparison of Jabulani and Brazuca non-spin aerodynamics. Proc Inst Mech Eng Part P J Sports Eng and Tech 2014;228:188-194.
[2] Chandler H, Controversy over new World Cup ball, CNN online, 3 June 2010.
[3] Lewis M, Official World Cup ball, Jabulani getting the blame for soft goals – Robert Green – and missed ones, New York Daily News, 14 June 2010.
[4] Asai T and Seo K. Aerodynamic drag of modern soccer balls. SpringerPlus 2013;2:171-175.
[5] Hong S and Asai T. Effect of panel shape of soccer ball on its flight characteristics. Scientific Reports 2014;May:1-7.
[6] Goff JE. A review of recent research into aerodynamics of sport projectiles. Sports Eng 2012;16:137-154.
[7] Myers T and Mitchell S. A mathematical analysis of the motion of an in-flight soccer ball. Sports Eng 2013;16:29-41.
[8] Choppin S. Calculating football drag profiles from simulated trajectories. Sports Eng 2013;16:189-194.
[9] Kray T, Franke J, and Frank W. Magnus effect on a rotating soccer ball at high Reynolds numbers. J Wind Eng & Ind Aero 2013;124:46-53.
[10] Lluna E, Santiago-Pradera V, Peris-Fajarnés G, and Defez B. Measurement of Aerodynamic Coefficients of Spherical Objects Using an Electro-optic Device. IEEE T Instrum & Meas 2013;62:2003-2009.
[11] Achenbach E. Experiments on the flow past spheres at very high Reynolds numbers. J Fluid Mech 1972;54:565-575.
[12] White FM. Fluid Mechanics, 7th edn. McGraw-Hill Higher Education, New York, New York; 2011.
[13] Schewe G. On the force fluctuations acting on a circular cylinder in crossflow from subcritical up to transcritical Reynolds numbers. J Fluid Mech 1983;133:265-285.
[14] Schewe G. Sensitivity of transition phenomena to small perturbation in flow around a circular cylinder. J Fluid Mech 1986;172:33-46.
[15] Daish CB. The Physics of Ball Games. The English Universities Pres Ltd, London; 1972.
[16] Gregory S, What's Wrong with the World Cup Ball?, Time online, 4 June 2010.
[17] `https://www.youtube.com/watch?v=k1YK0e-UWNg` (accessed 20 August 2014).
[18] Goff JE and Carré MJ. Soccer lift coefficients via trajectory analysis. Eur J Phys 2010;31:775-784.
[19] Goff JE and Carré MJ. Trajectory analysis of a soccer ball. Am J Phys 2009;77:1020-1027.
[20] Hong S and Asai T. Unsteady aerodynamic force on a knuckle ball in soccer. Japan J of Phys Ed, Health and Sport Sci 2010;55:553-563.
[21] Hong S and Asai T. Aerodynamics of Knuckling Effect Shot Using Kick-robot. Int J of App Sports Sciences 2011;23:406-420.
[22] Asai T and Kamemoto K. Flow structure of knuckling effects in footballs. J Fluids & Struc 2011;27:727-733.
[23] Ito S, Kamata M, Asai T, and Seo K. Factors of unpredictable shots concerning new soccer balls. Proc Eng 2012;34:152-157.